

Circular Dichroism of Neutral Zinc Porphyrin–Oligonucleotide Conjugates Modified with Flexible Linker

Akira Onoda,[2,†] Masahiro Igarashi,[1] Satoshi Naganawa,[1] Kiyomi Sasaki,[1] Shinya Ariyasu,[1] and Takeshi Yamamura*[1]

[1]Faculty of Science, Tokyo University of Science, 1-3 Kagurazaka, Shinjuku-ku, Tokyo 162-8601

[2]Department of Applied Chemistry, Graduate School of Engineering, Osaka University, 2-1 Yamadaoka, Suita, Osaka 565-0871

Received February 4, 2009; E-mail: tyamamur@rs.kagu.tus.ac.jp

Neutral zinc porphyrin containing flexible alkyl linker, 5-[4-(5-hydroxypentyloxy)phenyl]-10,15,20-tri-*p*-tolylporphyrinatozinc, was attached to the 5′ ends of 20- and 30-bp oligodeoxynucleotides (ODN) by solid-phase synthesis. Zinc porphyrin-modified double-stranded DNA (dsDNAs), which included dsDNAs with porphyrin moieties on one end and on both ends (ZnPor–ds20, ds20–ZnPor, ZnPor–ds20–ZnPor, ZnPor–ds30, ds30–ZnPor, and ZnPor–ds30–ZnPor), were successfully prepared and were analyzed by variable-temperature UV–vis spectroscopy and CD measurements to elucidate the interaction behavior of the porphyrin ring. Detailed investigation revealed that the zinc porphyrin–DNA conjugates exhibited intra-duplex porphyrin–ODN interaction in a low-salt condition and inter-duplex porphyrin–porphyrin interaction in a high-salt condition.

Porphyrins can serve as useful probe molecules in the structural studies on biomolecules because of their exciton chirality.[1–6] Based on the measurements of circular dichroism (CD), porphyrins and metalloporphyrins have been employed in conformational and configurational investigation of biomolecules, such as peptides,[7–9] oligosaccharides,[10] glycol lipids,[11] and the marine neurotoxin brevetoxin B.[12–14]

As the demonstration of the photosensitized cleavage of a nucleic acid with a interacting porphyrin moiety,[15–17] a variety of positively charged porphyrins and metalloporphyrins with bulky aryl groups at the meso position have been shown to bind to single-[18,19] and double-stranded DNA[20–23] (ssDNA and dsDNA, respectively). At the same time, some studies demonstrated the application of CD signals of porphyrin chromophores in carrying out conformational analyses of DNA molecules by noncovalent-[24] and covalent-modification strategies.[25–28] For example, a study reported the use of a zinc porphyrin as a chiroptical probe for the identification of B- and Z-DNA.[24] Covalent modification of DNAs with phenyltrispyridylporphin and their analogs by using a rigid amide linker also enabled the sensitive detection of conformational transition of oligodeoxynucleotides (ODNs) between B- and Z-DNA; this detection is due to the long-range exciton-coupled CD signal that is generated by the interaction between the two terminal porphyrins—with the distance between them reaching up to 40–50 Å[25,26]—attached to the 5′ ends of the DNA. On the ther hand, modification of ODNs with flexible linker has been carried out in studies conducted on DNA cleaving activity,[29] electron-transfer property,[30] and thermal stability of duplexes.[31]

Modification of porphyrin moiety via flexible linker will provide not only intra-strand interaction but also inter-strand interaction, which can be expanded to DNA–porphyrin assemblies. The flexible linkages can lead to exciton-coupled chirogenesis in porphyrin–DNA systems via three possible interactions: intra-duplex short-range exciton interaction between a porphyrin and a nucleic acid, intra-duplex long-range exciton interaction between the terminal porphyrins, and intermolecular exciton interaction between two porphyrins or between a porphyrin and a nucleic acid. Neutral porphyrins are less potential to interact with anionic DNA and favorable for assembling with other porphyrin molecules. The DNA conjugate having zinc porphyrin arrays in a close distance within a duplex studied recently.[32,33] To investigate the interactions with the zinc porphyrin both in the intra-strand and in the inter-strand, we synthesized series of zinc porphyrin-modified ODNs at 5′ end which comprise 20-bp and 30-bp dsDNAs having a porphyrin moiety attached at both ends or at each 5′ end of the DNA via a flexible linker (Figure 1 and Scheme 1). Herein, we report the studies on the CD signals of the zinc porphyrin–ODN conjugates to elucidate the type of interaction that is dependent on salt concentration.

Results and Discussion

Synthesis of Zinc Porphyrin ODNs. Zinc porphyrin ODNs were synthesized by the scheme shown in Figure 2. Zinc tetraarylporphyrin with C5 linker (**1**) was attached to the 5′ end of ODN by carrying out solid-support synthesis. The zinc porphyrin was O-phosphitylated by undergoing a coupling reaction with 2-cyanoethyl diisopropylphosphoramidochloridite, which was used immediately after purification. In

† Present address: Frontier Research Base for Global Young Researchers, Graduate School of Engineering, Osaka University, 2-1 Yamadaoka, Suita, Osaka 565-0871

Published on the web October 8, 2009; doi:10.1246/bcsj.82.1280

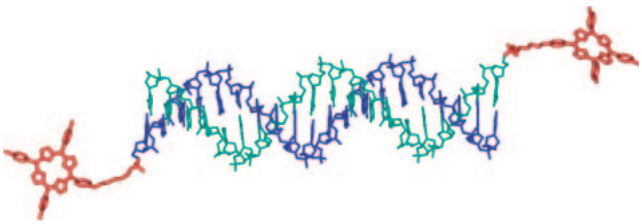

Figure 1. dsDNA molecule with porphyrin moieties at 5′ end with flexible linker.

ZnPor-ss20T

ZnPor-5'-GACATATGGGGCGATTACAG-3'

ss20B-ZnPor

3'-CTGTATACCCCGCTAATGTC-5'-ZnPor

ZnPor-ss30T

ZnPor-5'-GACTTATGGGGCGATGTTCCAGCAATACAG-3'

ss30B-ZnPor

3'-CTGAATACCCCGCTACAAGGTCGTTATGTC-5'-ZnPor

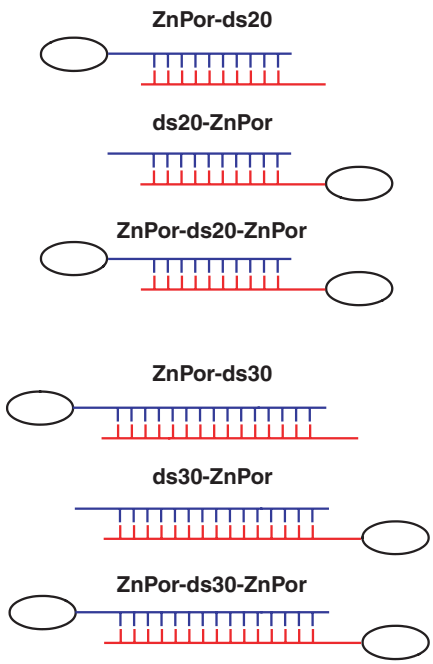

Scheme 1. Attachment of ZnPor moiety to ss- and dsDNA.

general, the corresponding phosphoramidite of a metal-free porphyrin is easily over oxidized to yield an unreactive phosphate. However, the phosphoramidite of zinc porphyrin is relatively stable after purification. The phosphoramide prepared above was coupled to the ODN on a controlled pore glass (CPG) resin used as a solid support. After cleavage and deprotection, the crude modified ODNs were purified by semi-preparative reverse-phase HPLC. The final product was characterized by matrix-assisted laser-desorption ionization time-of-flight (MALDI-TOF) MS. The UV–vis spectroscopy of the products confirmed the successful covalent modification of

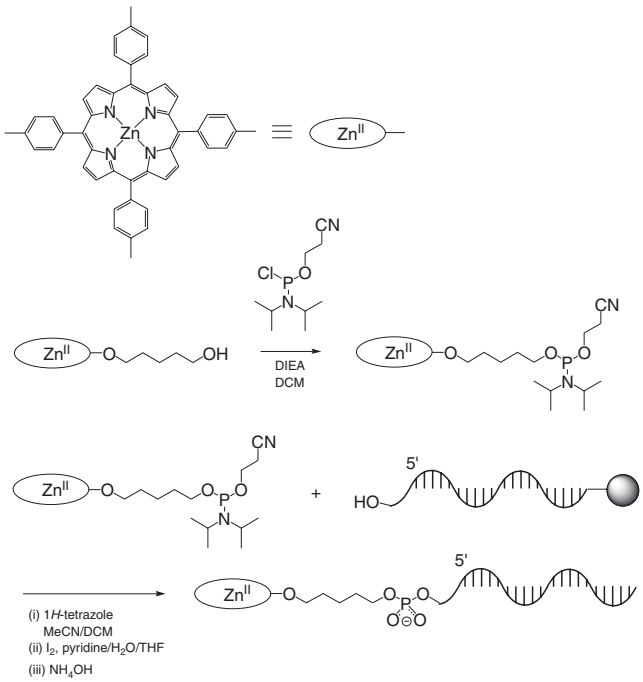

Figure 2. Synthesis of ODN containing Zn porphyrin at 5′ end.

the 20-bp and 30-bp ODNs by porphyrin (ZnPor–ss20T, ZnPor–ss20B, ZnPor–ss30T, and ss30B–ZnPor), the results of which are shown in Figure 3. Each product showed the characteristic Soret and Q bands of zinc porphyrin moieties at 430 nm and 560 and 600 nm, respectively; the intensities of these bands were proportional to that of the characteristic band of ODNs at 260 nm.

Variable-Temperature UV–Vis Spectroscopy. The results of the variable-temperature experiments suggest that the synthesis of singly and doubly modified DNA strands with porphyrin ring via C5 linker allows duplex formation. Figure 4 shows the variable-temperature UV–vis spectra of ZnPor–ds20, ds20–ZnPor, and ZnPor–ds20–ZnPor. The absorption maxima of these modified duplexes found at the same wavenumber shift in both the nucleic acid and porphyrin region. As the temperature increased, the band at 260 nm of the modified duplexes was observed to exhibit a typical hyperchromic shift, which was also observed in the spectra of porphyrin-free dsDNA. The Soret band at around 430 nm showed only a slight shift or increase in intensity on heating. The absorption spectra measured after carrying out the denaturation and renaturation of modified dsDNAs exhibited spectral features identical to those mentioned above indicating that the zinc–porphyrin modification did not interfere with the formation of the duplexes; this was observed in the case of all modified dsDNAs. The T_m value of the porphyrin-conjugated duplexes was slightly lower than that of the unmodified duplexes. It is known that an increase in T_m indicates an increase in the stability of the double helix, which is attributed to the intercalation of the porphyrin moiety.[20,34] Thus, we have verified that despite its hydrophobic nature the pendant porphyrin moiety does not directly bind to the dsDNA via processes such as intercalation or groove binding.

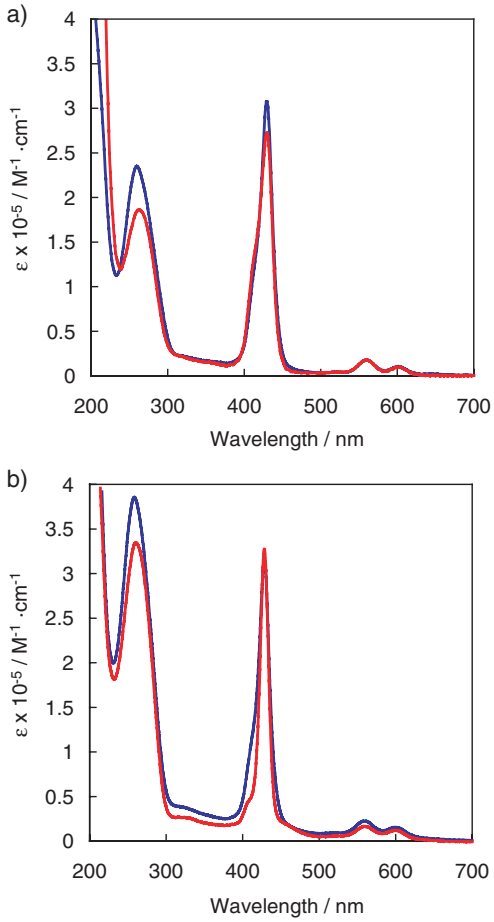

Figure 3. UV–vis spectra of (a) ZnPor–ss20T (blue) and ss20B–ZnPor (red) and (b) ZnPor–ss30T (blue) and ss30B–ZnPor (red) in aqueous solution.

The remarkable feature in our ZnPor-conjugated duplex is a gradual increase of OD260 during the melting profiles. The ds20 with similar DNA sequence gave a typical transition around T_m (44.5) in 0 mM NaCl. In contrast, ZnPor–ds20 and ds20–ZnPor showed a smooth increase which is more prominent in doubly modified ZnPor–ds20–ZnPor. This trend is more obvious in the higher salt concentration, 100 mM NaCl (Figure S4). The UV–vis analyses for the modified DNAs did not indicate that the zinc porphyrins were not involved in the strong interaction between the nucleobases. Weak interactions with the zinc porphyrin moieties were investigated by the following CD analyses.

CD Studies on Porphyrin-Conjugated dsDNAs. By carrying out CD experiments, we can elucidate the structural aspects of DNA strands and their electronic interaction with the porphyrin moiety. The appearance of CD bands in the Soret-band region indicates the existence of electronic interaction of the porphyrin chromophore with other chromophores, such as nucleobases or the other porphyrin ring. First, we performed CD measurements on different concentrations of the DNA conjugates and found that this electronic interaction originates mainly from intra-duplex interaction in a low-salt condition and that the effect of inter-duplex interaction is also apparent in a high-salt condition on our system. The CD profile of different concentrations of ZnPor–ds20–ZnPor is shown in Figure 5. The modified duplexes exhibited negative (245 nm) and positive (275 nm) CD bands characteristic of B-type DNA,[35] and the spectral features of the modified duplexes were identical to those observed in the case of the unmodified duplex. In the CD profile of the low-concentration sample, a strong positive band at 444 nm and relatively weak bands at around 420 nm were observed. Spectral changes observed in the case of higher sample concentration were analyzed by measuring difference spectra (Figure 5b); these spectra revealed that the changes at 415 and 425 nm are induced by the inter-duplex interaction. The relatively small change in CD bands is presumably caused by inter-duplex porphyrin–porphyrin interaction. Such spectral change due to the inter-duplex interaction could not be observed in low NaCl concentration. In higher salt concentration, the interaction between hydrophobic aromatic molecules is known to become stronger. Thus, our ZnPor-conjugated DNA is thought to give inter-strand porphyrin–porphyrin interaction.

The intra-duplex interaction was also assessed by CD measurements in a low-salt condition as shown in Figure 6. Each modified duplex exhibited different spectral features; the spectra of ZnPor–ds20, ds20–ZnPor, and ZnPor–ds20–ZnPor showed positive CD bands near 425, 436, and 444 nm, respectively. Further, it should be noted that we used non-palindromic ODN sequence in the synthesis of dsDNA. Therefore, the CD results suggest that the pendant porphyrin with C5 linker attached to the 5′ end of the DNA exhibits a different porphyrin–nucleotide interaction at each terminus of the duplex. CD spectra in the Soret-band region of the singly and doubly modified porphyrin–DNA conjugates were compared against each other to estimate the interaction behavior of the porphyrin moiety in the two types of conjugates. Figure 6a shows the CD profiles of ZnPor–ds20, ds20–ZnPor, and ZnPor–ds20–ZnPor, while the bottom figure shows the CD profile of ZnPor–ds20–ZnPor along with the combined spectrum of ZnPor–ds20 and ds20–ZnPor in Figure 6c. CD profile of ZnPor–ds20–ZnPor showed a strong positive band at 436 nm and a weak negative band at 425 nm, which are almost identical to the bands observed in the combined spectrum of the two singly modified dsDNAs. These results clearly indicate that porphyrin–ODN interaction at each terminus of the duplex is different from each other. It has been previously reported that some porphyrin chromophores that are fixed rigidly on both termini of the dsDNA exhibit long-range porphyrin–porphyrin exciton interaction.[25,26] However, in the case of our modified dsDNAs, the zinc porphyrins attached to the DNA via flexible linkers do not exhibit porphyrin–porphyrin exciton interaction but exhibit interaction with nucleotides localized at the termini.

Variable-temperature CD experiments with porphyrin-conjugated 20-bp and 30-bp duplexes, ZnPor–ds20–ZnPor and ZnPor–ds30–ZnPor, in the high-salt condition are shown in Figure 7. The CD bands at 415 and 425 nm assigned to the intermolecular ZnPor/ZnPor interactions are more prominent in ZnPor–ds30–ZnPor. The results indicated that the longer double-stranded DNA is more advantageous for the intermolecular ZnPor/ZnPor interaction at both termini.

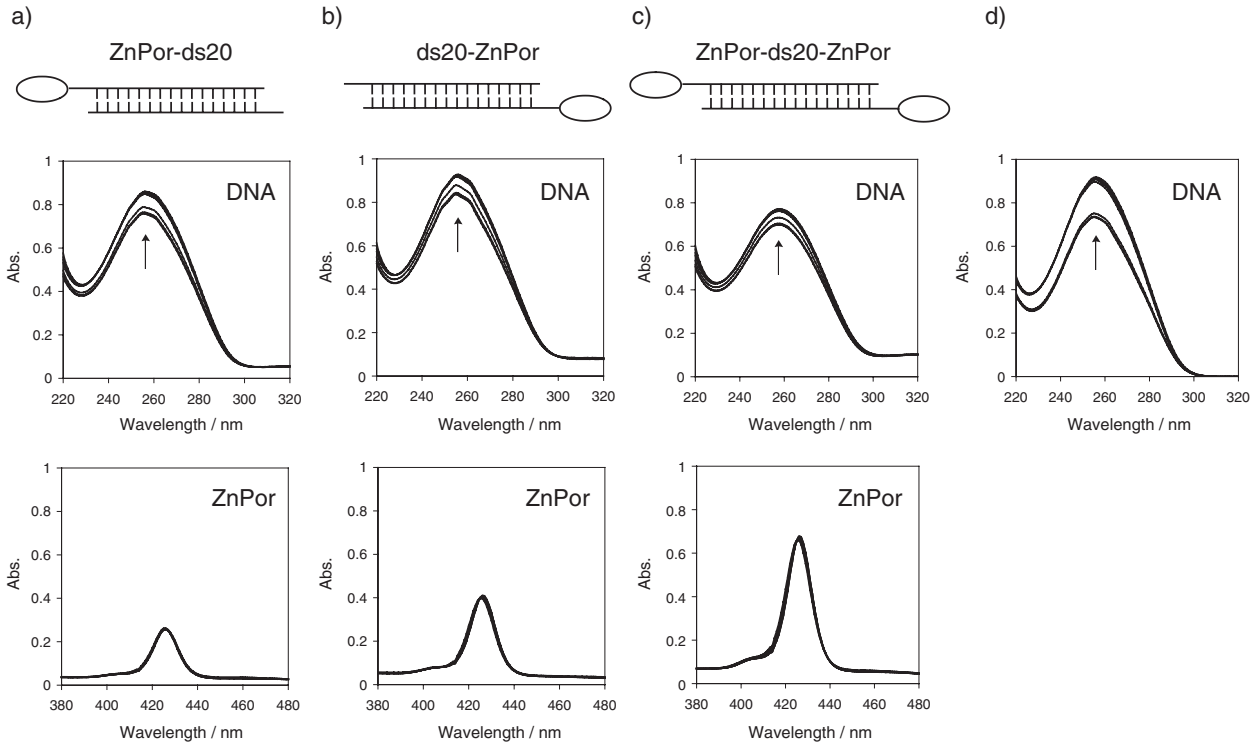

Figure 4. Variable-temperature absorption spectra of (a) ZnPor–ds20, (b) ds20–ZnPor, (c) ZnPor–ds20–ZnPor, and (d) ds20. The spectra were measured for 2 μM samples in 10 mM Tris-HCl solutions at 20, 30, 40, 50, 60, 70, and 80 °C.

Conclusion

We have synthesized zinc porphyrin–DNA conjugates using flexible alkyl linker and analyzed the interaction behavior of the porphyrin moieties in these conjugates by carrying out UV–vis spectroscopy and CD measurements. The results of the detailed investigation suggested that the neutral zinc porphyrin attached to the 5′ end of dsDNA exhibited intra-duplex zinc porphyrin–ODN interaction under low-salt condition and inter-duplex zinc porphyrin/zinc porphyrin under high-salt condition. The intermolecular interaction of our ZnPor-conjugated DNA led to form an aggregated species insoluble to an aqueous solution. The strategy attaching a neutral zinc porphyrin moiety with flexible linker provides responsive behavior in the pattern of the interaction between the porphyrins and the DNA duplexes.

Experimental

Materials. All solvents were distilled over appropriate drying agents and degassed prior to use. All starting reagents used were of commercial grade. H_2por-OCOEt (5-[4-(propionyloxy)phenyl]-10,15,20-tri-*p*-tolylporphin) was synthesized by following a previously reported procedure with some modifications.[36]

5-[4-(Propionyloxy)phenyl]-10,15,20-tri-*p*-tolylporphin (H_2por-OCOEt). 4-Propionyloxybenzaldehyde (10.0 g, 56.2 mmol), *p*-tolualdehyde (21.8 g, 181 mmol), and pyrrole (15.0 mL, 217 mmol) were dissolved in 44 mL of propionic acid and 22.4 mL of acetic anhydride. The mixture was refluxed for 2 h untill the solution turned dark purple in color. The reaction mixture was cooled to room temperature and concentrated to a volume of approximately 200 mL. The solution was made to stand overnight at −15 °C to afford crystalline precipitates. These precipitates were collected and dissolved in $CHCl_3$ for purification by using a silica gel column ($CHCl_3$:hexane = 7:3); this purification process was repeated twice. The collected fraction was dried in vacuo to obtained the final product. Yield, 3.5 g (4.1%). ^{1}H NMR ($CDCl_3$, 500 MHz): δ 8.85–8.83 (8H, m, β-pyrrole), 8.21 (2H, d, J = 8.5 Hz, ArH), 8.1 (6H, d, J = 7.5 Hz, ArH), 7.55 (6H, d, J = 7.5 Hz, ArH), 7.48 (2H, d, J = 8.5 Hz, ArH), 2.78 (2H, q, J = 7.6 Hz, CH_2), 2.70 (9H, s, CH_3), 1.41 (3H, t, J = 8.0 Hz, CH_3), −2.78 (2H, s, NH). MALDI-TOF MS m/z calcd for $C_{50}H_{41}N_4O_2$ [M + H$^+$]: 729.32, found 728.97.

5-[4-(5-Hydroxypentyloxy)phenyl]-10,15,20-tri-*p*-tolylporphin (H_2por-C_5H_{10}OH). H_2por-OCOEt (400 mg, 0.56 mmol) was dissolved in 12 mL of DMF added to NaOH (720 mg, 17 mmol), and the solution was stirred for 2 h at room temperature. This mixture was added to 5-bromopentyl acetate (144 μL, 9.2×10^{-1} mmol), and the solution was stirred for 4 h. This mixed solution was neutralized by adding 1 M HCl to obtain the product, H_2Por-C_5H_{10}OCOMe, which was extracted using $CHCl_3$. The organic layer was washed with aqueous $NaHCO_3$ solution and then with water, and the collected filtrate was evaporated to dryness. The residue was dissolved in 22 mL of DMF and hydrolyzed by adding 5 M NaOH. The reaction mixture was neutralized, the product was extracted with $CHCl_3$, and the organic phase was washed with water. The product was purified by column chromatography ($CHCl_3$:MeOH = 95:5) and recrystallized by $CHCl_3$–hexane solvent mixture to give H_2por-C_5H_{10}OH. Yield, 419 mg (98%). ^{1}H NMR ($CDCl_3$, 500 MHz): δ 8.85–8.83 (8H, m, β-pyrrole), 8.10–8.07 (8H, m, ArH), 7.55 (6H, d, J = 7.5 Hz, ArH), 7.21 (2H, d, J = 7.5 Hz, ArH), 4.26 (2H, t, J = 6.4 Hz, CH_2), 3.78 (2H, td, J = 6.4, 5.0 Hz, CH_2), 2.70 (9H, s, CH_3), 2.01 (2H, tt, J = 6.4, 7.5 Hz, CH_2), 1.81–1.69 (4H, m, CH_2), −2.78 (s, 2H, NH). MALDI-TOF MS m/z calcd for $C_{52}H_{47}N_4O_2$ [M + H$^+$]: 759.37, found 758.07.

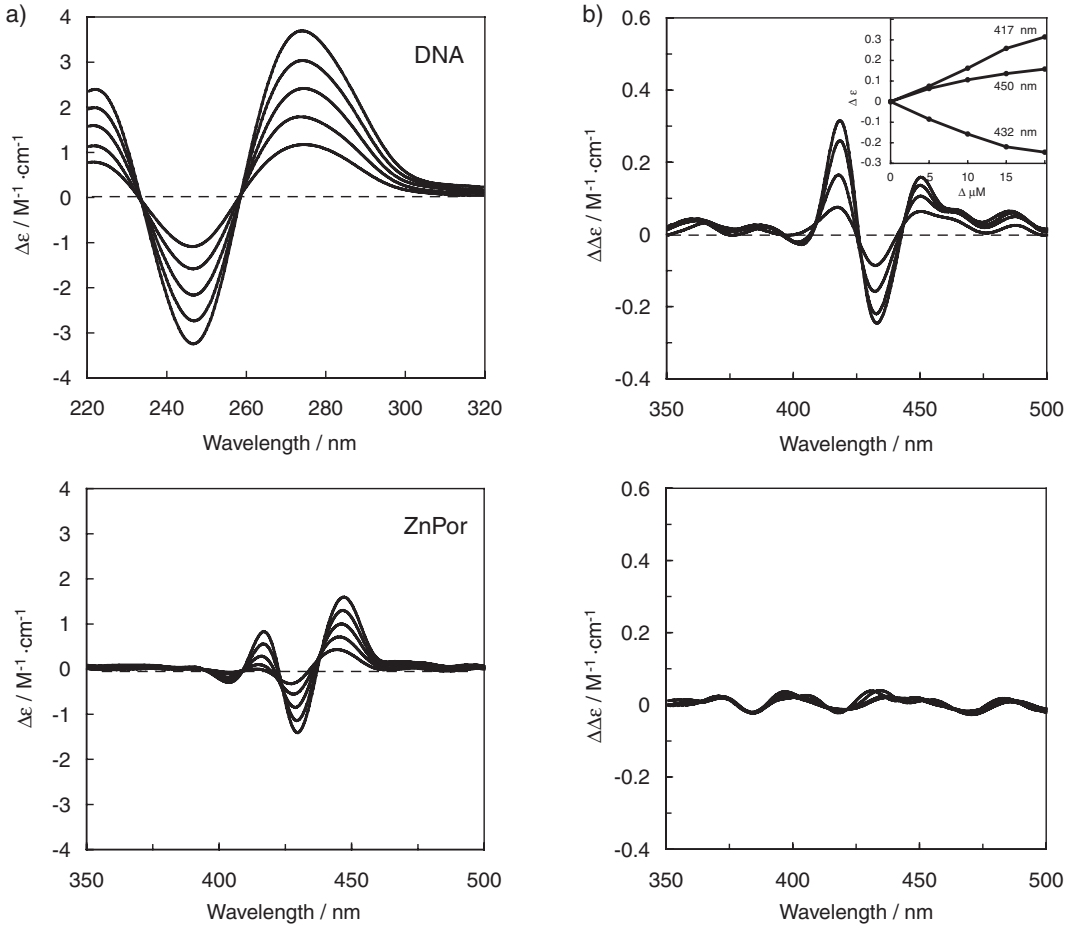

Figure 5. (a) Concentration-dependent CD spectra of ZnPor–ds20–ZnPor in 10 mM Tris-HCl, 1 mM EDTA, and 100 mM NaCl solutions. The spectra were measured at sample concentrations of 10, 15, 20, 25, and 30 μM. Top; 220–320 nm, Bottom; 350–500 nm. (b) Difference spectra at each sample concentration of 10, 15, 20, 25, and 30 μM. 10 mM Tris-HCl, 1 mM EDTA, and 100 mM NaCl solutions (top) and 10 mM Tris-HCl (bottom). The inset shows the intensity profile at 417, 432, and 450 nm.

5-[4-(5-Hydroxypentyloxy)phenyl]-10,15,20-tri-*p*-tolylporphininatozinc (Znpor-$C_5H_{10}OH$) (1). H_2por-OH (100 mg, 0.13 mmol) and Zn(acac)$_2$ (115 mg, 4.4 mmol) were dissolved in 12 mL of $CHCl_3$–MeOH solvent ($CHCl_3$:MeOH = 9:1). The reaction mixture was stirred for 1 h. Then, the reaction solution was washed with water, and the organic layer was collected and evaporated to dryness. The residue was purified by using a silica gel column ($CHCl_3$:MeOH = 95:5) and recrystallized to give blue purple powder of **1**. Yield, 90 mg (83%). The successful incorporation of Zn^{2+} ion in the porphyrin ring was verified by absorption spectroscopy. ^{1}H NMR ($CDCl_3$, 500 MHz): δ 8.88–8.67 (8H, m, β-pyrrole), 8.04–8.01 (8H, m, ArH), 7.47 (6H, d, J = 7.6 Hz, ArH), 7.21 (2H, d, J = 6.7 Hz, ArH), 4.20 (2H, t, J = 6.4 Hz, CH_2), 3.63 (2H, td, J = 6.4, 5.0 Hz, CH_2), 2.64 (9H, s, CH_3), 1.94 (2H, tt, J = 6.4, 7.5 Hz, CH_2), 1.69–1.60 (4H, m, CH_2). MALDI-TOF MS m/z calcd for $C_{52}H_{44}N_4O_2Zn$ [M + H$^+$]: 821.28, found 821.10.

Znpor Phosphoramidite. 2-Cyanoethyl diisopropylphosphoramidochloridite (0.5 M in CH_2Cl_2) (24 μL, 0.0012 mmol) and DIEA (*N*,*N*-diisopropylethylamine) (3.9 μL, 0.0024 mmol) were dissolved in 0.5 mL of CH_2Cl_2, and after degassing, the solution was mixed with Znpor-$C_5H_{10}OH$ (**1**) (5.0 mg, 0.0061 mmol). The reaction mixture was stirred for 1 h in Ar atmosphere protected form light. The reaction was monitored by TLC (silica gel) using 5% triethylamine (TEA) in hexane–ethyl acetate solvent (hexane:ethyl acetate = 1:1). During this chromatography, the solution was concentrated and charged into a silica gel column, which was eluted with 5% TEA in the hexane–ethyl acetate solvent. The purified band was evaporated to give a bluish purple powder of ZnPor phosphoramidite. The purified product was used immediately in the solid-phase coupling reaction. ^{31}P NMR ($CDCl_3$): δ 147.4 ppm. ^{1}H NMR ($CDCl_3$, 500 MHz): δ 8.88–8.85 (8H, m, β-pyrrole), 8.03 (2H, d, J = 8.7 Hz, ArH), 8.02 (6H, d, J = 7.6 Hz, ArH), 7.47 (6H, d, J = 7.6 Hz, ArH), 7.27 (2H, d, J = 8.7 Hz, ArH), 4.19 (2H, t, J = 6.4 Hz, CH_2), 3.87–3.60 (4H, m, CH_2), 3.60–3.54 (2H, m, *i*Pr-CH), 2.63 (9H, s, CH_3), 2.60 (2H, t, J = 6.4 Hz, CH_2), 1.95 (2H, tt, J = 6.4, 7.8 Hz, CH_2), 1.78–1.72 (2H, m, CH_2), 1.69–1.64 (2H, m, CH_2), 1.18–1.14 (12H, m, *i*Pr-CH_3).

Synthesis of Porphyrin-Modified ODNs. To the ODN, which was supported on the CPG resin, ca. 4 mM CH_2Cl_2 solution of porphyrin phosphoramidite (300 μL) was added with 0.1 M acetonitrile solution of tetrazole (200 μL) in Ar atmosphere. The reaction vessel was stirred for 2 h in the absence of light at room temperature. This procedure was repeated twice. Then, the mixture was washed with CH_2Cl_2 and acetonitrile five times, and 21 mL of the oxidizing agent I_2 (0.15 M, H_2O:pyridine:THF = 10:10:1) was added to the solution and the mixture was stirred for 2 min. The solution was filtered and the solid support was washed with acetonitrile five times. The porphyrin-modified resin was dissolved

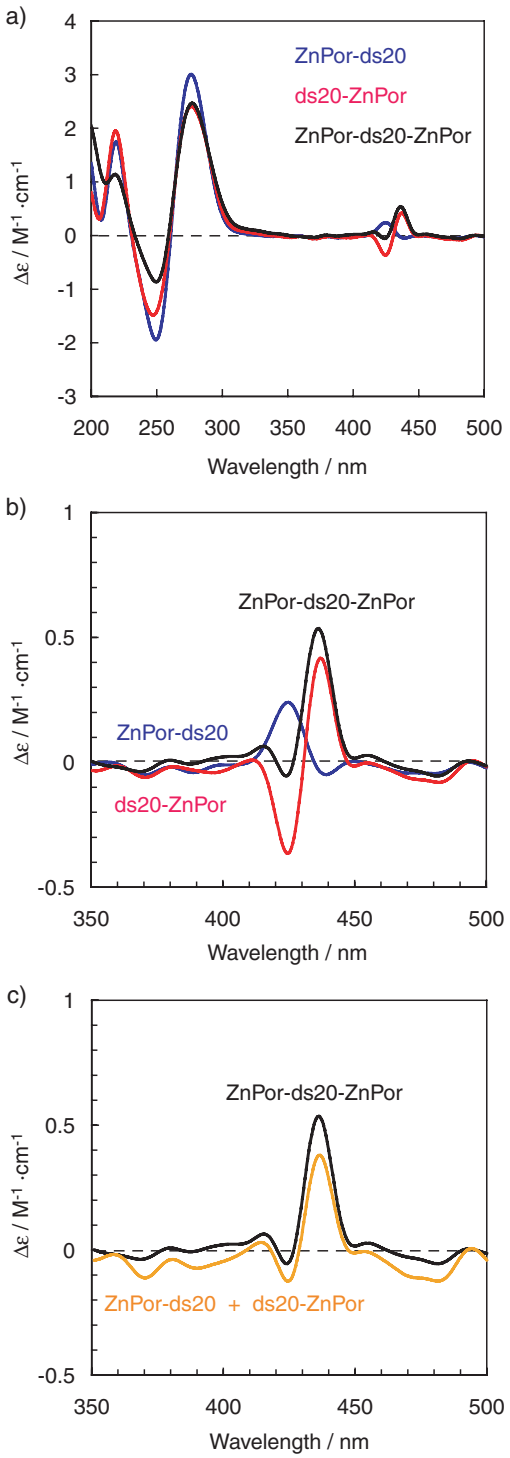

Figure 6. (a) and (b) CD spectra of ZnPor–ds20–ZnPor (black), ZnPor–ds20 (blue), and ds20–ZnPor (red) in 10 mM Tris-HCl solution. (c) The spectrum of ZnPor–ds20–ZnPor along with the combined spectrum of ZnPor–ds20 and ds20–ZnPor (orange).

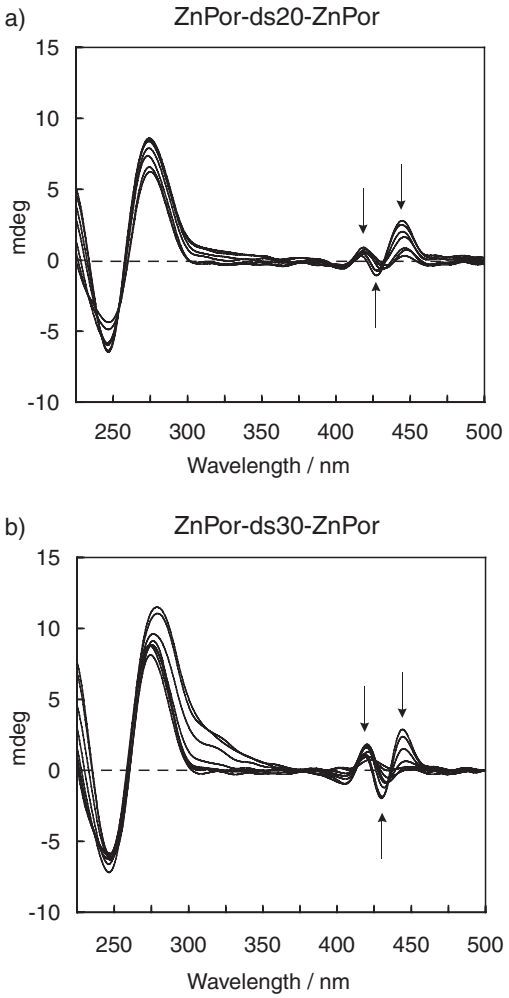

Figure 7. Variable-temperature CD spectra of (a) ZnPor–ds20–ZnPor and (b) ZnPor–ds30–ZnPor. The spectra were measured for 20 μM samples in 10 mM Tris-HCl, 1 mM EDTA, and 100 mM NaCl solutions at 20, 30, 40, 50, 60, 70, and 80 °C.

in 5 mL of 28% ammonia solution, and the mixture was stirred for 15 h at 55 °C. The reaction mixture was concentrated to dryness, and the obtained residue was dissolved in H_2O, while the cleaved solid support was filtered off. The products were purified on C18 reverse-phase HPLC column with a gradient of acetonitrile:0.1 M tetraethylammonium acetate (TEAA) (1:4–4:1).

MALDI-TOF MS. Zn^{II}Por–ss20T, found 7080, calcd 7069; ss20B–Zn^{II}Por, found 6897, calcd 6891; Zn^{II}Por–ss30T, found 10272, calcd 10262 (+7Na); ss30B–Zn^{II}Por, found 10033, calcd 10041 (+2Na). Negative ion mode with CHCA matrix.

Physical Measurements. The ^{1}H NMR spectra were measured using a JEOL JNM-LA500 or Bruker AVANCE 600 spectrometer. The ^{31}P NMR spectra were measured using the JEOL JNM-LA500 spectrometer. ^{1}H NMR spectra were measured using TMS as an internal reference standard, and ^{31}P spectra were measured using 85% aqueous H_3PO_4 as an external reference standard. The UV–vis spectra were recorded on a Shimadzu UV-2200A spectrophotometer. The UV melting experiments were carried out using a Beckman Coulter DU 800 spectrophotometer. The fluorescence spectra were recorded on a Shimadzu RF5300-PC fluorescence spectrometer. The CD spectra were measured on a Jasco J-725 spectropolarimeter. The MALDI-TOF MS experiments were performed using PerSpective Biosystems Voyager LinerRD VDA-500, and the electrospray ionization time-of-flight (ESI-TOF) MS experiments were performed using Bruker micrOTOF spectrometer.

We greatly acknowledge Prof. Hidetaka Torigoe for permitting us to carry out UV melting experiments. This study was supported by a Grant-in-Aid for Scientific Research (No. 1835034 to T.Y. and 16750148 to A.O.) from the Ministry of Education, Culture, Sports, Science and Technology, Japan.

Supporting Information

^{1}H and ^{31}P NMR spectra of ZnPor–$C_5H_{10}OH$ phosphoramide. MALDI-TOF MS, UV–vis, CD, and fluorescence spectra. This material is available free of charge on the web at: http://www.csj.jp/journals/bcsj/.

References

1 N. Berova, K. Nakanishi, R. W. Wood, *Circular Dichroism: Principles and Applications*, 2nd ed., Wiley-VCH, New York, **2000**.

2 K. Harada, K. Nakanishi, *Circular Dichroic Spectroscopy: Exciton Coupling in Organic Stereochemistry*, Oxford University Press, Oxford, **1983**, p. 304.

3 K. Harada, K. Nakanishi, *Acc. Chem. Res.* **1972**, *5*, 257.

4 X. Huang, B. H. Rickman, B. Borhan, N. Berova, K. Nakanishi, *J. Am. Chem. Soc.* **1998**, *120*, 6185.

5 X. Huang, K. Nakanishi, N. Berova, *Chirality* **2000**, *12*, 237.

6 G. Pescitelli, S. Gabriel, Y. Wang, J. Fleischhauer, R. W. Woody, N. Berova, *J. Am. Chem. Soc.* **2003**, *125*, 7613.

7 H. Mihara, Y. Haruta, S. Sakamoto, N. Nishino, H. Aoyagi, *Chem. Lett.* **1996**, 1.

8 S. Oancea, F. Formaggio, S. Campestrini, Q. B. Broxterman, B. Kaptein, C. Toniolo, *Biopolymers* **2003**, *72*, 105.

9 T. Arai, N. Inudo, T. Ishimatsu, T. Sasaki, T. Kato, N. Nishino, *Chem. Lett.* **2001**, 1240.

10 F. X. Redl, M. Lutz, J. Daub, *Chem.—Eur. J.* **2001**, *7*, 5350.

11 J. B. MacMillan, T. F. Molinski, *J. Am. Chem. Soc.* **2004**, *126*, 9944.

12 S. Matile, N. Berova, K. Nakanishi, S. Novkova, I. Philipova, B. Blagoev, *J. Am. Chem. Soc.* **1995**, *117*, 7021.

13 S. Matile, N. Berova, K. Nakanishi, *Chem. Biol.* **1996**, *3*, 379.

14 S. Matile, N. Berova, K. Nakanishi, J. Fleischhauer, R. W. Woody, *J. Am. Chem. Soc.* **1996**, *118*, 5198.

15 B. R. Munson, R. J. Fiel, *Nucleic Acids Res.* **1992**, *20*, 1315.

16 D. R. McMillin, K. M. McNett, *Chem. Rev.* **1998**, *98*, 1201.

17 S. Mettath, B. R. Munson, R. K. Pandey, *Bioconjugate Chem.* **1999**, *10*, 94.

18 M. J. Carvlin, R. J. Fiel, *Nucleic Acids Res.* **1983**, *11*, 6121.

19 R. F. Pasternack, R. A. Brigandi, M. J. Abrams, A. P. Williams, E. J. Gibbs, *Inorg. Chem.* **1990**, *29*, 4483.

20 R. J. Fiel, J. C. Howard, E. H. Mark, N. Datta Gupta, *Nucleic Acids Res.* **1979**, *6*, 3093.

21 R. J. Fiel, B. R. Munson, *Nucleic Acids Res.* **1980**, *8*, 2835.

22 R. F. Pasternack, E. J. Gibbs, J. J. Villafranca, *Biochemistry* **1983**, *22*, 2406.

23 M. A. Sari, J. P. Battioni, D. Dupré, D. Mansuy, J. B. Le Pecq, *Biochemistry* **1990**, *29*, 4205.

24 M. Balaz, M. De Napoli, A. E. Holmes, A. Mammana, K. Nakanishi, N. Berova, R. Purrello, *Angew. Chem., Int. Ed.* **2005**, *44*, 4006.

25 M. Balaz, A. E. Molmes, M. Benedetti, P. C. Rodriguez, N. Berova, K. Nakanishi, G. Proni, *J. Am. Chem. Soc.* **2005**, *127*, 4172.

26 M. Balaz, B. C. Li, J. D. Steinkruger, G. A. Ellestad, K. Nakanishi, N. Berova, *Org. Biomol. Chem.* **2006**, *4*, 1865.

27 M. Balaz, J. D. Steinkruger, G. A. Ellestad, N. Berova, *Org. Lett.* **2005**, *7*, 5613.

28 M. Balaz, A. E. Holmes, M. Benedetti, G. Proni, N. Berova, *Bioorg. Med. Chem.* **2005**, *13*, 2413.

29 B. Mestre, A. Jakobs, G. Pratviel, B. Meunier, *Biochemistry* **1996**, *35*, 9140.

30 M. Endo, T. Shiroyama, M. Fujitsuka, T. Majima, *J. Org. Chem.* **2005**, *70*, 7468.

31 K. Berlin, R. K. Jain, M. D. Simon, C. Richert, *J. Org. Chem.* **1998**, *63*, 1527.

32 L.-A. Fendt, I. Bouamaied, S. Thöni, N. Amiot, E. Stulz, *J. Am. Chem. Soc.* **2007**, *129*, 15319.

33 M. Endo, M. Fujitsuka, T. Majima, *J. Org. Chem.* **2008**, *73*, 1106.

34 P. Lugo-Ponce, D. R. MacMillin, *Coord. Chem. Rev.* **2000**, *208*, 169.

35 D. M. Gray, F. D. Hamilton, M. R. Vaughan, *Biopolymers* **1978**, *17*, 85.

36 C. Casas, B. Saint-Jalmes, C. Loup, C. J. Lacey, B. Meunier, *J. Org. Chem.* **1993**, *58*, 2913.